CHIN. PHYS. LETT. Vol. 27, No. 4 (2010) 043301

Theory of Tunnel Ionization in Complex Systems *

ZHANG Bin(张斌), ZHAO Zeng-Xiu(赵增秀)**

Department of Physics, National University of Defense Technology, Changsha 410073

(Received 17 September 2009)

We present a detailed derivation of the Ammosov–Delone–Krainov theory of tunnel ionization in complex systems (CS-ADK). A few mistakes in the previous works have been found and corrected. The theory is then applied to CO_2, showing that CS-ADK yields better agreement with experiment than the molecular ADK theory.

PACS: 33. 80. Rv, 42. 50. Hz DOI: 10.1088/0256-307X/27/4/043301

Tunnel ionization of atoms and molecules in an intense laser field have been investigated extensively in the last decades. The so-called Ammosov–Delone–Krainov (ADK) model[1] provides for many atomic species a very good description of measured total ionization rates. For molecules, Tong *et al.*[2] generalized the basic model of the ADK theory for atoms to the diatomic molecular ADK theory (MO-ADK), which was further generalized to also account for nonlinear multi-atom molecules by Kjeldsen *et al.*,[3] and some reasonable results as compared to experiments have been reported. The ADK/MO-ADK theory is based on the single active electron (SAE) approximation, where only the weakest bound valence electron interacts with the laser. This model becomes less applicable when SAE approximation fails.[4] Theoretical predictions from the ADK theory often overestimate experimentally measured ionization yields by orders of magnitude. Recent years, a quasi-analytical multi-electron model of tunnel ionization of complex systems (CS-ADK) was developed,[4–6] revealing that the SAE approximation loses its validity in complex materials. This model opens the door to explore the new multi-electron physics associated with tunnel ionization in complex systems. In this Letter, first a detailed derivation of the CS-ADK theory is presented. We introduce a correlated strong-field (CSF) ansatz,[6] which takes into account the long-range interaction between the tunnel and core electrons. A single effective electron (SEE) equation for the tunnel is derived and solved quasi-analytically. Secondly, we validate this theory by applying it to CO_2, a hotspot in recent studies.[7–10] The results are compared with the MO-ADK theory and experiment, and a detailed discussion is presented.

We first review and summarize the derivation of the SEE equation for tunnel ionization of previous works.[4–6] Tunnel ionization takes place in the quasi-static limit, i.e., the laser remains constant during the tunnel process. Therefore, the derivation starts from the time-independent n-electron Schrodinger equation (atomic units are used unless otherwise indicated),

$$-I_n\,\Psi_n = \Big[\sum_{j=1}^{n}(H_j - \boldsymbol{r}_j\cdot\boldsymbol{E}) + V_{ee}^n\Big]\,\Psi_n, \qquad (1)$$

where $H_j = T_j + V_j$ denotes the field free single-electron Hamiltonian of the jth electron with $T_j = -(1/2)\nabla_j^2$, and V_j represents the attractive potential due to the nuclei. The second term in Eq. (1) represents the electron laser dipole interaction with $\boldsymbol{E} = -\boldsymbol{z}E$. The repulsive interaction potential of the n electrons is $V_{ee}^n = \sum_{k<j}^{n} 1/|\boldsymbol{r}_k - \boldsymbol{r}_j|$. The laser dressed wave function and total energy of the n-electron ground state are denoted by $\Psi_n(\boldsymbol{r}_1,\cdots,\boldsymbol{r}_n)$ and I_n respectively. Second order perturbation theory yields $I_n = \tau_n - (1/2)\beta_n E^2$ with τ_n the free total energy and β_n the polarizability tensor component along $\boldsymbol{E}$.

Equation (1) is solved by using the CSF ansatz $\Psi_n(\boldsymbol{r}_r,\boldsymbol{r}) = \Psi_{n-1}(\boldsymbol{r}_r,\boldsymbol{r})\otimes\Psi_t(\boldsymbol{r})$, where Ψ_{n-1} is the ground state of the ionized system in the combine fields of laser and escaping electron; Ψ_t denotes the wavefunction of the tunnel electron (assigned the coordinate $\boldsymbol{r} = \boldsymbol{r}_n$); and $\boldsymbol{r}_r = (\boldsymbol{r}_1,\cdots,\boldsymbol{r}_{n-1})$ refers to the residual bound electrons. The neglect of anti-symmetrization between tunnel and core electrons in the CSF ansatz is valid asymptotically for $|\boldsymbol{r}| \gg |\boldsymbol{r}_r|$. Further, V_{ee} can be expanded to the second order in $|\boldsymbol{r}|$, yielding $V_{ee}^n = V_{ee}^{n-1} + (n-1)/|\boldsymbol{r}| + \sum_{j=1}^{n-1}\boldsymbol{r}_j\cdot\boldsymbol{d}$. Here V_{ee}^{n-1} denotes the interaction between the $n-1$ core electrons, $\boldsymbol{d} = (\boldsymbol{r}/|\boldsymbol{r}|^3) \approx \boldsymbol{z}d$ and $d = 1/z^2$.

Following the molecular Born–Oppenheimer derivation, Eq. (1) can be decoupled into two equations, separating Ψ_{n-1} and Ψ_t. The bound electron part satisfies

$$-I_{n-1}\,\Psi_{n-1} = \Big[\sum_{j=1}^{n-1}(H_j - z_j E_t) + V_{ee}^{n-1}\Big]\,\Psi_{n-1}, \quad (2)$$

where $I_{n-1} \approx \tau_{n-1} - (1/2)\beta_{n-1}E_t^2$ is the total energy of the electronic ground state of the ionized medium dressed by the combined laser and tunnel electron

*Supported by the National Natural Science Foundation of China under Grant Nos 10676039 and 10874245, the National Basic Research Program of China under Grant No 2007CB815105, and the National High-Tech ICF Committee in China.

**Email: Zhaozengxiu@gmail.com

field, $E_t = E - d$. The total energy of the field-free electronic state is τ_{n-1}, and β_{n-1} is the polarizability.

The equation for the tunnel electron is

$$-(I_n - I_{n-1})\,\Psi_t = \Big(\langle T\rangle - \frac{Z_c}{|\boldsymbol{r}|} - zE\Big)\,\Psi_t, \qquad (3)$$

where Z_c is the charge of parent ion after ionization. The first term, $\langle T\rangle = \langle \Psi_{n-1}|T|\,\Psi_{n-1}\rangle$, contains an integration over $d^3\boldsymbol{r}_r$. The kinetic operator is applied with respect to $\boldsymbol{r}$ yielding $\nabla^2\,\Psi_{n-1}\,\Psi_t = \Psi_{n-1}\nabla^2\,\Psi_t + 2\nabla\,\Psi_{n-1}\nabla\,\Psi_t + \Psi_t\nabla^2\,\Psi_{n-1}$. Similar to the Born–Oppenheimer theory the second and third terms can be neglected. The perturbation theory shows that they contribute to higher order multipole terms. The energy divergence in Eq. (3) can be written as $I_n - I_{n-1} = I_p + (1/2)[\beta_{n-1}E_t^2 - \beta_n E^2]$ with $I_p = \tau_n - \tau_{n-1}$ being the field-free ionization potential. As the change of polarizability due to the removal of a single electron is generally small, we can set $\beta_n \approx \beta_{n-1} = \beta_+$. Then we obtain $I_n - I_{n-1} \approx I_p + \nabla I_p$ with $\nabla I_p \approx -\beta_+ E/z^2 + \beta_+/2z^4$.

With the above approximations, Eq. (3) becomes

$$I_p\,\Psi_t = \Big(\frac{1}{2}\nabla^2 - V(\boldsymbol{r}) + zE\Big)\,\Psi_t,$$
$$V(\boldsymbol{r}) = -\frac{Z_c}{|\boldsymbol{r}|} + \frac{\beta_+ E}{z^2} - \frac{\beta_+}{2z^4}. \qquad (4)$$

Equation (4) generalizes ADK/MO-ADK from the SAE theory to the SEE theory, which describes the tunnel ionization in complex materials. The interaction between core and ionizing electrons is accounted for by β_+, the dominant contribution of the polarizability tensor along the laser electric field. Further, in standard ionization theories[1–3] the (angular momentum-) l-barrier $(l+1/2)^2/r^2$ is neglected. As complex systems can have large l values, this effect must be accounted in in this study.

Now we present the detailed derivation of the solution of the SEE equation of our work. Equation (4) is solved in two limits: inside the tunnel barrier, where laser field effects are weak and the l-barrier is most pronounced and outside the barrier, where the laser field dominates and the l-barrier is negligible. The two solutions are connected in the intermediate area (under the barrier).

The solution inside the barrier starts from spherical coordinates, $r = |\boldsymbol{r}|, \theta, \varphi$. As only parts of the wavefunction in a narrow cone along the laser electric field, $\theta \approx 0$, contribute to tunnel ionization, the solution can be greatly simplified. Using $\cos\theta \approx 1$, angular and radial parts of Eq. (4) are decoupled and the solution can be written as $\Psi_t(\boldsymbol{r}) = \sum_{lm}\psi_{lm}(\boldsymbol{r}) = \sum_{lm} Y_{lm}(\theta,\varphi)F_l(r)$. The spherical harmonics are approximated by the leading term

$$Y_{lm} \approx \frac{Q_{lm}}{(2\pi)^{1/2})2^{|m|}|m|!}\sin^{|m|}\theta\exp(im\varphi),$$
$$Q_{lm} = (-1)^m\Big(\frac{(2l+1)(l+|m|!)}{2(l-|m|!)}\Big)^{1/2}. \qquad (5)$$

As the laser field effects are weak in this region, $F_l(r)$ is approximated by the asymptotic form of Coulomb wave function $F_l(r) \approx C_{lm}r^{Z_c/k-1}e^{-kr}$. Here $\psi_{lm}(\boldsymbol{r})$ is Fourier transformed to the coordinate system z, p, ϕ by

$$\psi_{lm}(z,p,\phi) = \frac{1}{2\pi}\iint \psi_{lm}(\boldsymbol{r})\exp\Big(ik_x x + ik_y y\Big)dxdy, \qquad (6)$$

which gives

$$\psi_{lm}(z,p,\phi) = \frac{C_{lm}Q_{lm}p^{|m|}z^{Z_c/k}\exp[im(\phi+\pi/2)]}{\sqrt{2\pi}2^{|m|}|m|!k^{1+|m|}\exp(\sqrt{k^2+p^2}z)}, \qquad (7)$$

where p and φ determine the momentum transversal to $\boldsymbol{z}$.

Table 1. Asymptotic coefficients for HOMO1 of CO2 (Data are from Ref. [7]).

L	m	C_{lm}
2	±1	±1.27
4	±1	±0.188
6	±1	±0.014

The solution under and outside the barrier is solved by the WKB method.[11] The semiclassical wave function in the classically forbidden region $z < z_1$ is an exponentially decreasing function of z

$$\psi_{lm}^{\rm WKB}(z,p,\phi) = \frac{C}{\sqrt{|p_z|}}\exp\Big(-\int_{z_1}^{z}|p_z|dz\Big), \qquad (8)$$

with $p_z = [k^2 + p^2 + 2(V(z) + (l+1/2)^2/z^2 - Ez)]^{1/2}$ the momentum along $\boldsymbol{z}$ and $k^2 = 2I_p$. The lower integration limit z_1 is the outer turning point at which $p_z = 0$, which for $z \gg 1$ is seen to be $z_1 \approx k^2/2E$. The semiclassical solution in the classically allowed region $z > z_1$ is a running-wave solution

$$\psi_{lm}^{\rm WKB}(z,p,\phi) = \frac{C}{\sqrt{|p_z|}}\exp\Big(i\int_{z_1}^{z}|p_z|dz - i\frac{\pi}{4}\Big). \qquad (9)$$

The laser dressed tunnel wavefunction (8) is matched to the field-free, asymptotic ground state (7) at a field-free point z_0,

$$C = \frac{D_{lm}Q_{lm}p^{|m|}\exp[im(\phi+\pi/2)]}{\sqrt{2\pi}2^{|m|}|m|!k^{1/2+|m|}}\exp\Big(-\int_{z_0}^{z_1}|p_z|dz\Big), \qquad (10)$$

where $D_{lm} = C_{lm}z_0^{Z_c/k}e^{-kz_0}$. As complex systems are highly polarizable, the polarization field cancels the laser field at a point a, where $\beta_+ E/a^2 - aE \approx 0$. Solution of this equation gives $z_0 = a = \beta_+^{1/3}$.

Finally the total wavefunction outside the barrier is

$$\Psi_t = \sum_l \frac{A_l}{(2\pi|p_z|)^{1/2}}\exp\Big(-\int_{z_0}^{z_1}|p_z|dz\Big),$$
$$A_l = \sum_m \frac{D_{lm}Q_{lm}p^{|m|}}{2^{|m|}|m|!k^{1/2+|m|}}\exp[im(\phi+\pi/2)]. \qquad (11)$$

Note that a factor $\exp\left(i\int_{z_1}^{z}|p_z|dz - i\pi/4\right)$ in Ψ_t has been neglected since the l-barrier can be neglected in the region $z > z_1(\gg 1)$, and Ψ_t only enters the final expression for the ionization rate as $|\Psi_t|^2$. Ionization along an arbitrary direction can be calculated by a rotation of the coordinate system by the Euler angle $\boldsymbol{R}$, keeping $\boldsymbol{E} \parallel \boldsymbol{z}$. This determines $B_{lm} = \sum_{m'} D^l_{m'm}(\boldsymbol{R})Q_{lm'}D_{lm'}$, which substitutes $D_{lm}Q_{lm}$ in A_l.

From Eq. (11) the tunnel current $j_z = |\Psi_t|^2 p_z$ is

$$j_z = \frac{1}{2\pi}\Big|\sum_l A_l \exp\Big[-t - \big(\frac{p}{\Delta}\big)^2\Big]\Big|, \qquad (12)$$

where $t = \int_{z_0}^{z_1} p_{z0}dz$, $p_{z0} = p_z(p=0)$ and $1/\Delta^2 = \int_{z_0}^{z_1} 1/p_{z0}dz$. Both t and Δ are closely l-dependant. Note that Eq. (12) corrects a mistake in Eq. (7) of Ref. [6]. Finally, the ionization rate is obtained by performing the integral $W = \int d\phi dp p j_z$, which gives

$$W = \sum_m \frac{1}{(2k)^{2|m|+1}|m|!}\Big|\sum_l B_{lm}e^{-t}\Delta^{(|m|+1)}\Big|^2. \qquad (13)$$

Equation (13) corrects Eq. (8) of Ref. [6]. In a slowly varying field, the ionization rate is found by integrating over an optical cycle. Under the assumption $k^3/E \gg 1$, the result is

$$W \approx \big(\frac{3E}{\pi k^3}\big)^{1/2}\frac{W^+ + W^-}{2}, \qquad (14)$$

where $W^{\pm}$ are the static rates for the positive and negative field directions with respect to the $\boldsymbol{z}$ direction. $W^+ = W$, and we have to substitute $(-1)^l C_{lm}$ for C_{lm} in B_{lm} to obtain W^-.[3]

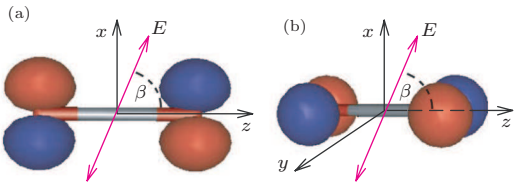

Fig. 1. (Color online) The orientation (β) of the two degenerate HOMO orbitals of CO_2 with respect to the linearly polarized field.

We validate the CS-ADK theory by applying it to CO_2. The ionization potential (I_p) and polarizability along the main axis are 13.777 eV and 2.507 A^3, respectively. These data are taken from the CCCBDB DataBase of NIST.[12] HOMO of CO_2 has the π_g symmetry and is a doubly degenerate orbital. For convenience we call them HOMO1 (on x–z plane, Fig. 1(a)) and HOMO2 (on y–z plane, Fig. 1(b)). The coefficients C_{lm} are determined by matching $F_{lm}(r) = \int Y^*_{lm}(\theta,\varphi)\Phi_0(\boldsymbol{r})d\Omega$ to the form $C_{lm}r^{(Z_c/k)-1}e^{-kr}$ in the asymptotic region.[13] In this study we adopt the C_{lm} values suggested in Ref. [7] (listed in Table 1 for HOMO1 of CO_2). For the total ionization rate of HOMO, we must sum up the rates from each degenerate orbital. We must only calculate the coefficients for HOMO1 of CO_2. HOMO2 has the same electron density distribution as HOMO1, except for lying on a different plane (Fig. 1). We obtain HOMO2 when HOMO1 is rotated by the Euler angle $\boldsymbol{R}_1(0,0,\pi/2)$. Thus the ionization rate of HOMO2 is $W(F, \boldsymbol{R}+\boldsymbol{R}_1)$ and the total ionization rate is

$$W_T(F,\boldsymbol{R}) = W(F,\boldsymbol{R}) + W(F,\boldsymbol{R}+\boldsymbol{R}_1). \qquad (15)$$

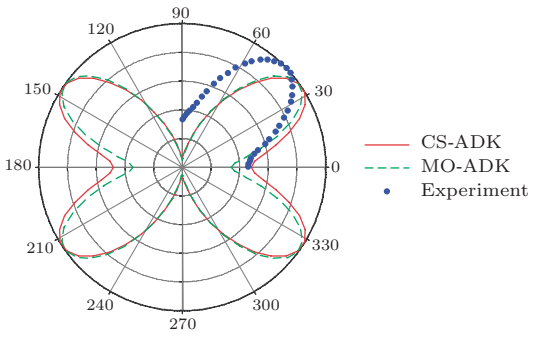

Fig. 2. (Color online) Normalized ionization probability of CO_2 versus the relative orientation β between the molecular axis and the laser polarization. The Laser intensity is 3×10^{13} W/cm^2, and the wavelength is 800 nm. The experimental data are taken from Ref. [8].

The ionization rates have to be converted to ionization probability or ion signal if we want to compare the calculation with experiment. The ionization rate depends on the instantaneous amplitude of the field and the molecular orientation described by the Euler angles (α,β,γ). We only consider linearly polarized light and hence the results are independent of α, the angle of rotation around the polarization vector. For a Gaussian laser beam with the vector potential $A(\mathcal{R},\mathcal{Z},t)$, the orientational dependent number of ionized molecules N is found by integrating over the beam profile $N(\beta,\gamma) = 2\pi\rho\int\int \mathcal{R}d\mathcal{R}d\mathcal{Z}p(\mathcal{R},\mathcal{Z},\beta,\gamma)$, where $p = 1-\exp[-\int W_T(A(\mathcal{R},\mathcal{Z},t),0,\beta,\gamma)dt]$ is the ionization probability and ρ the constant density of the target gas. In experiments it is difficult to measure the absolute yield due to unknown detection efficiency, while measured ratios of yields for different molecular orientations are independent of detection efficiency.

In Fig. 2 we present the ionization probabilities of CO_2, versus the relative orientation β (see Fig. 1). The angle where the ionization probability peaks from the experiment[8] is 45°, while both the CS-ADK and MO-ADK predict the peaks at about 35°. Although such discrepancies exist, the alignment dependences of ionization rates predicted using those theories are still correct, at least quantitatively, as far as the simplicity and approximate nature are considered. Further, careful observation shows that the angular distribution from CS-ADK differs from that of MO-ADK, especially when the C – O axis parallels to the polarization direction of laser field ($\beta = 0°$, 180°), where a

shallower gap is found. In this sense, the result from CS-ADK is closer to experimental data. In experiments, utilizing linearly polarized pulses for the alignment, the main axis with the largest polarizability is aligned along the polarization direction[14] (C − O axis for CO_2). Figure 3 shows the theoretical results of the ionization rates versus the laser intensity when CO_2 is aligned. It is well known that the predictions from ADK theory often over estimate experimentally measured ionization yields by orders of magnitude.[6] In Fig. 3 we can see that the result from the CS-ADK theory improves the situation, especially when the intensity increases.

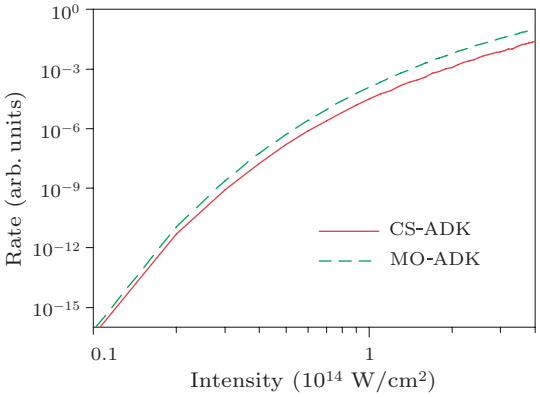

Fig. 3. (Color online) Ionization rates of CO_2 versus the laser intensity when the C − O axis is aligned along the laser field polarization.

Recall that the CSF approach takes into account: (1) the long-range interaction potential $V_p = \beta_+ E/z^2 - \beta_+/2z^4$ and (2) the angular momentum l-barrier $V_l = (l+1/2)^2/r^2$. CS-ADK degenerates into MO-ADK if these two potentials are taken away. Now we study how these two factors affect our results. Figure 4(a) presents the ionization rates versus the Euler angle β, calculated from CS-ADK, CS-ADK*(no polarizability, $\beta_+ = 0$) and MO-ADK, respectively. CS-ADK* differs from MO-ADK by considering the contribution from V_l, while CS-ADK differs from CS-ADK* by V_p. We notice an obvious change in the ionization rate when compare the results from CS-ADK* and MO-ADK. This means that the l-barrier changes both the angular distribution and amplitude. Meanwhile, V_l is always > 0, so the tunnel barrier rises and the electron is harder to be ionized, resulting in the decreases in yield rate. On the other hand, the comparison between CS-ADK and CS-ADK* tells us that the interaction potential V_p affects the magnitude (decrease in this case) but not the angular distribution of yield results. In fact, if we plot the two results from CS-ADK and CS-ADK* in one polar graph (normalize to the $\beta = 0°$ geometry first), we will find that these two curves totally overlap (as Fig. 2). This originates from the neglect of the inhomogeneity nature of polarizability. In Fig. 4(b) we present the V_p potential, with the typical values of our calculation (the field strength $E \ll 1$, the tunnel region $z > 1$). As the field strengthens, V_p tends to increase in the asymptotic region, which further raises the tunnel barrier. This explains the decreases of ionization yield from CS-ADK calculation in Fig. 4(a).

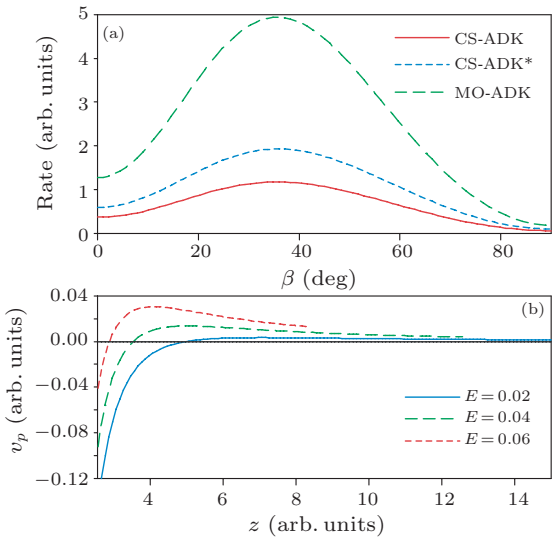

Fig. 4. (Color online) (a) Ionization rate of CO_2 versus the relative orientation β between the molecule and the laser polarization. The laser intensity is 6×10^{13} W/cm^2. (b) Interaction potential V_p at different field strengths.

In conclusion, we have reviewed the theory of tunnel ionization in complex systems. The CS-ADK theory improves the MO-ADK theory by taking into account the interaction between the tunnel electron and the remaining electrons bound to the ion core and as well as the angular momentum barrier. Comparison of the theory to the MO-ADK theory shows that better agreement with experiment is reached. A data basis with a variety of parameters including the polarizability is needed to make it more generally applicable. In future work, it will be a breakthrough if the electronic exchange-correlation effect is successfully introduced into this theory.

References

[1] Ammosov M V et al 1986 *Sov. Phys. JETP* **64** 1191
[2] Tong X M et al 2002 *Phys. Rev.* A **66** 033402
[3] Kjeldsen T K et al 2005 *Phys. Rev.* A **71** 013418
[4] Brabec T et al 2005 *Phys. Rev. Lett.* **95** 073001
[5] Zhao Z X and Brabec T 2006 *J. Phys.* B **39** L345
[6] Zhao Z X and Brabec T 2007 *J. Mol. Opt.* **54** 981
[7] Zhao S F, Jin C and Le A T et al 2009 *Phys. Rev.* A **80** 051402(R)
[8] Thomann I et al 2008 *J. Phys. Chem.* A **112** 9382
[9] Yun L H, Jin C and Bing J H et al 2009 *Chin. Phys. Lett.* **26** 104207
[10] Sheng Z, Qin X Y and Quan W Y et al 2009 *Chin. Phys. Lett.* **26** 083202
[11] Bisgaard C Z and Madsen L B 2004 *Am. J. Phys.* **72** 249
[12] CCCBDB website: http://cccbdb.nist.gov/expdata.asp
[13] Kjeldsen T K and Madsen L B 2004 *J. Phys.* B **37** 2033
[14] Stapelfeldt H and Seideman T 2003 *Rev. Mod. Phys.* **75** 543